Coupling geochemical and geophysical signatures to constrain strain changes along thrust faults

R. Petrini[1], F. Italiano[2], A. Riggio[3], F.F. Slejko[1], M. Santulin[3], A. Buccianti[4], P. Bonfanti[2] and D. Slejko[3]

[1] Dipartimento di Geoscienze, Università di Trieste, Italy
[2] Ist. Naz. Geofisica e Vulcanologia, Palermo, Italy
[3] Ist. Naz. Oceanografia e Geofisica Sperimentale, Trieste, Italy
[4] Dipartimento di Scienze della Terra, Università di Firenze, Italy

ABSTRACT   Anomalous geochemical signals inferred from elemental and isotopic analyses on spring waters and soil degassing are often detected in response to tectonic loading along faults. Recent results highlighted how the geochemical anomalies are closely related to episodes of crustal deformation. In the present study, the carbon dioxide and radon from soil degassing and the geochemical features of springs spatially related to fault zones in the Friuli-Venezia Giulia region (north-eastern Italy), a seismic-prone area, have been coupled with crustal deformation analyses to better define the possible correlations between fluctuations of geochemical parameters and seismicity, with the aim of gaining new information about local geodynamic processes. The natural CO_2 and Rn degassing was evaluated by a soil gas survey carried out by a grid of about 100 measuring sites located over the area that had been hit by strong earthquakes, in the past (Gemona – Idrija 1511, Raveo 1700, Tolmezzo 1788 and 1928, Gemona 1976). The results obtained show a significant amount of crustal-originated gases, especially CO_2, possibly related to decarbonation reactions and stress accumulation occurring in deep-seated structures. The spring waters show, in some cases, anomalous geochemical transients, in particular concerning the chloride and Rn concentration, that are not related to seasonal changes and interpreted to reflect distinct fluid pressure regimes within the fault zone, yielding the leakage of pore fluids into the country-rock aquifers. In particular, the changes in the chloride content have been tentatively modeled in terms of pore-fluid expulsion from compacting clays during pressure gradients at shallow crustal levels. The flow regimes and chemical evolution have been related to the strain computed at the outlet sites through the Gutenberg–Richter relation parameters and the regional value of the strain rate. The information provided here may be used to start up a long-term geochemical monitoring of this seismically active area able to detect the modifications occurring in the circulating fluids to gain a better insight on the relationships between the geochemistry of the fluids and the activity of the local seismogenic faults.

1. Introduction

The seismic crisis that seriously damaged L'Aquila city and a large portion of the central Apennines caused a loss of human lives (more than 300) besides causing damage to social infrastructures and the cultural heritage, although a magnitude 6.3 earthquake cannot be considered a very strong event. The low building quality was the main reason for the vast destruction and damage, however the scientific world has again asked for more thorough investigations on all of the possible ways of mitigating earthquake damage including both prevention and prediction.

Due to the dimension of the problem of seismic hazard, the possibility of forecasting seismic events has always attracted all the people living in earthquake-prone areas, and many empirical methods were proposed in order to predict earthquakes. Apart from sporadic cases [e.g., the successfully forecasted Haicheng earthquake in 1975; Mogi (1985)] no other earthquakes have been forecasted, making the prediction a controversial matter of debate. Scholz *et al.* (1973) proposed that the precursory phenomena are more evident in heterogeneous materials and in tectonic regimes involving a significant thrust faulting component that allows high stress values. As such, the authors state that the reason why precursory phenomena failed in some areas and were successful elsewhere was the difference in the tectonic regime. Consequently, statistical approaches to seismic hazard assessment, the basis for seismic designing and building retrofitting, continue to offer the most cost-effective means of reducing earthquake-related losses.

On the other hand, in spite of the large amount of scientific work already done, there is still a lack of knowledge regarding the physical process responsible for earthquake generation. This observation implies that both statistical and physical methods have to be developed simultaneously: the former indicates, statistically, the areas with the highest probability of earthquake occurrence, the latter models the natural processes that develop during the preparatory phase of seismic events.

Several observations have shown that fluids are intimately linked to a variety of faulting processes, displaying temporal modifications as a consequence of the fault movements due to crustal deformation. A number of field observations suggest, in fact, that an interconnected system of fluid-filled cracks and a pore fluid honeycomb characterize the continental crust. In particular, tectonic settings such as in reverse steep faults (Sibson, 1990), a directional flow of these fluids within the fault meshes and shear fractures may be promoted in response to pressure gradients. It is expected that the chemistry of the fluids migrating through the seismogenic portions of a fault and discharged in proximity of the fault trace reflects the degree of completion of a number of reactions occurring between the lithologies under stress and the fluid phase (e.g., Toutain and Barbon, 1999; Pizzino *et al.*, 2004a, 2004b). In this sense, the fluid composition may become a probe of the interseismic and coseismic strain changes that characterize active faults, recording the interplay between the gauge and country-rocks in controlling their circulation in seismically active areas. In particular, transient geochemical modifications in feeder aquifers related to active regional tectonic structures can be recognized on the basis of thermodynamics and mass-balance calculations, starting from the physico-chemical properties, the solute content and their isotopic signatures.

This paper presents the results of a research activity carried out over the Friuli-Venezia Giulia region, one of the most seismic-prone areas in Italy, hit by strong earthquakes both in the past and

in recent times (Slejko *et al*., 1989). Soil degassing measurements associated with the geochemical features of the gas phase dissolved in waters at a regional scale highlighted the fact that a crustal-originated, CO_2-dominated phase is released through the tectonic structures of the region (Riggio *et al*., 2007; Italiano *et al*., 2009). As matter of fact, some previous studies concerning this region (Riggio and Sancin, 1986; Riggio *et al*., 2003) have indicated a possible relation between long period Rn variations and the *b*-value (Gutenberg and Richter, 1944) behaviour in time and space, suggesting thus that Rn degassing could be modulated by stress accumulation.

Low-temperature waters vented coinciding with the main tectonic lineaments show chemical compositions closely related to the geological formation crossed by the hydrologic circuits. The local tectonic lines play a major role in driving the circulation of the fluids because of an enhanced vertical permeability that allows the infiltrating waters to reach deep crustal layers, to equilibrate with the rocks of the aquifers and to rise up towards the surface through fault lines. Some of the waters have shown temporal changes in some geochemical features: the modifications are interpreted here following a new approach, aimed at closely understanding the details of the relationships between the crustal strain and the fluid behaviour. The geochemical anomalies, recorded by a mid-term monitoring activity, are compared to the computed accumulation in time of the strain which will be later released as earthquakes. Such an approach allows us to couple physical effects due to the tectonic activity, responsible for the strain accumulation, with the geochemical modifications induced by changes in rock properties before the rupture, namely before the occurrence of the earthquake.

2. Geo-tectonic outlines, seismicity and spring location

The eastern sector of the Southern Alps has been affected by the thrusting which forms the orogenic structure of this sector of the Alps, dipping to the north (Carulli and Ponton, 1992). In particular, during the Alpine orogen (Neogene) in the Friuli-Venezia Giulia region the NW-SE-trending Dinaric thrusts underwent reactivation with crustal shortenings related to the Apulia-Europe collision and with the development of E-W and NE-SW embricated structures, mostly S-verging. During this compressive phase, tectonic units were detached over Permian and Triassic evaporite layers building ramp-and-flat carbonate structures (Carulli and Ponton, 1992; Merlini *et al*., 2002) which override mainly Paleocene-Eocene flysch formations.

Most of the springs sampled in this study are spatially related to these structures (Fig. 1), and are intended as representative of waters actively migrating along the fault planes. In particular, three of the water outlets are located along different segments of the Barcis-Staro Selo lineament, also referred to in the past as the Periadriatic overthrust (see Carulli *et al*., 2002). This structure places the Dolomia Principale (Norian) in tectonic contact over Eocene-Miocene terrigenous units, yielding a shortening of about 20 km (Merlini *et al*., 2002). The plane, N-dipping between 20° and 60°, is generally E-W oriented (Cavallin and Martinis, 1982) with some undulations and was restructured during Paleogene-Neogene post collisional events (neo-Alpine phases). In particular, the Barcis spring outflows along a S-dipping backthrust of the Barcis-Staro Selo line (Ponton, 2008).

Two springs among those studied are related to the Mt. Dof-Mt. Auda lineament, an E-W

oriented overthrust plunging to the north which juxtaposes Carnian and Norian dolomites on Jurassic and Cretaceous formations (Carulli *et al*., 2000) with a N-S shortening of a few kilometres.

One spring is located along the Alto Tagliamento lineament, which represents an E-W trending overthrust where the lower Carnian sedimentary sequence, overlapping the Dolomia Principale, is strongly folded toward the south, separating the northern sector of the Carnian Alps from the impinging southern edge.

Two springs are related to the Fella-Sava lineament and its prosecution westwards. The Fella - Sava line is a high-angle backthrust S-dipping reverse fault (Venturini, 1990), limiting the Julian Alps to the north and which juxtaposes Permo-Scitic carbonatic, silico-clastic deposits and evaporitic sequences to Mesozoic carbonate units composed by dolomitic limestones.

Finally, one of the springs is related to the Mt. Bernadia line, a system of Paleogenic Dinaric thrusts, involving the Cretaceous platform limestones and Eocenic torbidites.

In summary, the sampled groundwaters encompass both the eastern and western part of the Southern Alps in Friuli, including sectors differing in terms of tectonic regime: the western and central portion of the chain are interpreted as affected by a compressional state of stress, while a strike-slip state of stress is dominant in the eastern sector (Slejko *et al*., 1989; Bressan *et al*., 1998).

The above-mentioned structures are the result of an intense tectonic activity driven by the subduction of the Adria Plate beneath the Alpine-Dinaric belt. It is commonly accepted that the seismotectonics of the area are influenced by three main lithospheric units, the Adria and Tisza microplates and the Euroasia plate, whose relative motion causes an intense seismic activity with the occurrence of several destructive earthquakes (Gruppo di Lavoro CPTI, 1999, 2004). Among them, worthy of note the M_W 6.7 event that hit the present Italian-Austrian border area in 1348, the M_W 6.5 quake of 1511 at the present Slovenian-Italian border region, the event of M_W 5.8 that caused severe destruction in Raveo on July 28, 1700, the two events that struck Tolmezzo on October 20, 1788 and March 27, 1928, both with an M_W of 5.7, and the recent seismic sequence of 1976 that ruined several villages of central Friuli (Gemona, Trasaghis, Venzone, etc.) with the strong events of May 6, 1976 of M_W 6.4 and September 15 of M_W 5.9. It is worth noting that the two earthquakes of April 12, 1998 and July 12, 2004, with an M_W of 5.7 and 5.1 respectively (Gruppo di lavoro CPTI, 2004; OGS, 2000-2010), hit Bovec in Slovenian territory. The seismicity of the study area is summarized in Fig. 1b, where the epicentres of historical and recent earthquakes are reported. The subduction of the Adria microplate shortens the continental crust of the Southalpine region along a N-S direction where overthrusts move at a rate of about 2.5 mm/yr (Cheloni *et al*., 2004) and provokes a NE-SW extension at a rate of about 1-2.5 mm/yr (Poli, 1996; Zanferrari *et al*., 2003; Galadini *et al*., 2005). The subduction process is also responsible for the uplifting recorded over the whole area with some sudden accelerations. The last two occurred as coseismic deformations on May 6 and on September 15, 1976 inducing an uplift of about 15 mm over the Udine area, of 100 mm at Gemona, and of 180 mm at Venzone (Talamo *et al*., 1978).

3. Methods

3.1. Soil gas measurements

A 5,000 km^2 wide area was investigated for soil degassing. The measurements were carried
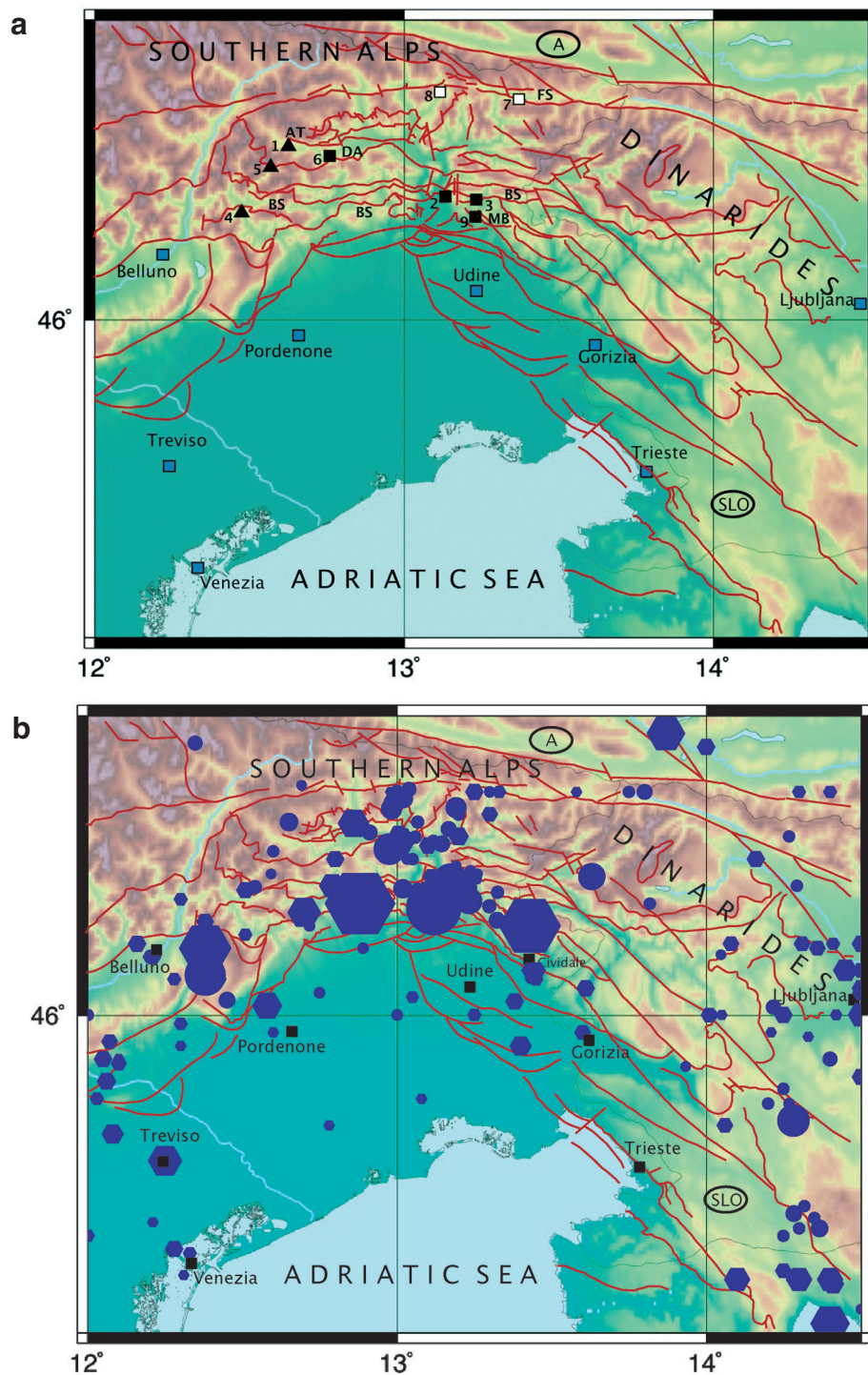
Fig. 1 - Sketch map of the study area: a) location of the sampling sites (hydrofacies: solid squares = Ca-Mg-HCO$_3$-type, open squares = Ca-Mg-SO$_4$-type, solid triangles = Ca-Mg-HCO$_3$-SO$_4$-type, according to the results shown in Fig. 4; the numbers refer to Table 1) and main tectonic lines (after Carulli, 2006); b) location of the epicentres of historical (solid hexagons for pre-1900 events) and recent (solid circles for post-1900 events) earthquakes of the area.

out over an almost regular grid with a 10-km step, following the dynamic concentration technique (Carapezza and Granieri, 2004; Italiano *et al.*, 2009). The method, originally developed to measure the soil CO_2 concentration in a gas mixture (Gurrieri and Valenza, 1988), was modified to measure the CO_2 and the Rn content of the soil gas simultaneously. The soil gas was driven by a pump with a calibrated and constant flow rate (we adopted 1 and 3 litres per minute) to an infra-red spectrometer for CO_2 and an equipment (ionization chamber and/or scintillation cell) for the Rn. The measuring devices were connected in series for a contemporaneous measurement of both gas species on the gas volume. The gas is pumped through a pipe of a section of 2.5 cm^2 inserted at a depth of about 50 cm in the soil. The CO_2 and Rn concentration values are taken when a constant value is reached, normally after 20 minutes of continuous pumping. As the survey was carried out over a long time span, a possible influence of variable meteorological conditions was considered. Changes in the atmospheric pressure, wind velocity and soil humidity may affect the actual gas flux. However, the adopted method of dynamic measurements overcomes some of these disturbances as the pipe sucks the gas 50 cm beneath the surface, where temperature, humidity and atmospheric pressure display smoother variations compared to shallower layers. Since the aim of the survey was to detect active degassing not to make mass output estimations, changes in the gas flow rate due to the above mentioned parameters do not affect the significance of our measurements.

The CO_2 and Rn concentrations are related to the flux by the relationship:

$$\phi_t = FCD \tag{1}$$

where ϕ_t is the gas flux, CD are the measured concentrations and F is the flow rate of the pump. Although a factor, mainly depending on the soil permeability should be adopted, our approach was aimed at looking for the presence of a positive soil gas flux towards the atmosphere. As such, only the flow rate of the pump and the gas concentrations were taken into consideration.

3.2. Computing strain at a site

Assuming that large earthquakes release all the strain that accumulates between earthquakes, in a simple elastic rebound model of an infinite strike-slip fault, material on the far right of the fault moves at the far-field rate *v* relative to the left side of the fault after an earthquake, thus it has moved a distance *vt* by time *t* (Stein and Wysession, 2003). However, between one earthquake and another, the fault is locked down to depth *W* (depth to which faulting extends), although it slips freely below, so material at the fault does not move between earthquakes. When the next large earthquake occurs, thus completing the seismic cycle, everything to the right of the fault has moved a distance *vt*. The coseismic slip is less than the slip across the fault except at the fault: so, points away from the fault have already moved part of the distance before the earthquake. A similar behaviour can be seen to the left of the fault.

Hence, during the interseismic period, material on the left side, near the locked fault, is pulled, only to rebound during the earthquake. Material on the right side, near the fault, is kept back during the interseismic period, only to move forward to the far-field motion due to the coseismic deformation.

The width of the zone across which the motion changes rapidly depends on the locking depth *W*: shallow locking makes the interseismic slip concentrate near the fault, whereas deeper locking
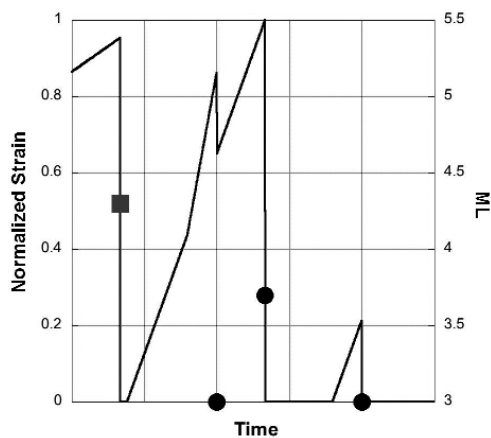
Fig. 2 - Normalized strain time history from a synthetic catalogue consisting of 4 earthquakes. Solid circles represent events with an epicentral distance less than 50 km from the studied site, the solid square indicates an event with a larger epicentral distance.

spreads it out towards a broad shear zone.

For a strike-slip fault, the interseismic shear strain rate can be obtained by:

$$\dot{e}_{xy} = \frac{ds(y)}{2dy} = \frac{v}{2\pi W \left[1 + \left(y/W \right)^2 \right]} \tag{2}$$

where $s(y)$ is the fault-parallel interseismic motion at the distance y from the fault (Stein and Wysession, 2003). Strain accumulates near the fault during the interseismic period and it is released in large earthquakes. Similarly to the displacement, the variation of strain with distance from the fault depends on the locking depth and far-field rate.

Although hydrogeochemical phenomena and Rn are considered strain indicators (e.g., Ulomov and Mavashev, 1971), the physical mechanism and their relationship with the strain are not yet well understood (Virk *et al*., 2000). It is hypothesized that micro-fractures in the deeper strata are created due to strain that increases the permeability of the strata (Sukhija *et al*., 2010). Consequently, fluid, gas, or electromagnetic measurements might detect deformation indirectly, albeit at localized sites and with amplitudes related nonlinearly to strain (Roeloffs, 1999).

In our study, strain at a site has been computed through the parameters of the Gutenberg–Richter (G-R) relation and the regional value of the strain rate. More precisely, the recurrence interval of the different magnitudes is obtained from the G-R relation and defines the time interval of strain build up in the region. The strain at the epicentral area on a certain day is obtained simply by multiplying the daily strain rate times the days of strain accumulation. This strain corresponds to the quantity given by Eq. (2) when y is 0. The reduction of the epicentral strain to the studied site is obtained by Eq. (2) when y is the epicentral distance. The time history of a synthetic case is illustrated in Fig. 2. Four earthquakes are considered: three are close to the studied site (i.e., epicentral distance less than 50 km) and have magnitude of 3.0, 3.7, and 3.0 one is far from the site and has a magnitude of 4.3.

The space distribution of strain can be computed similarly, by simply mapping the strain values computed on a regular grid for a certain date.

4. The Friuli experiment

4.1. Fluids: sampling and analytical procedures

Groundwaters were sampled during field surveys carried out between 2006 and 2010. The sample locations are listed in Table 1, with the corresponding associated lineament.

Water temperature, redox potential (Eh), pH, and electrical conductivity were measured in the field using a Simphony SP80PC portable instrument. Accuracy was ±0.2 °C for temperature, ±0.05 for pH; ±0.01 V for Eh and 1% for electrical conductivity. Eh was reported to the standard hydrogen electrode by contemporaneously measuring a ZoBell's solution. The HCO_3 content (i.e., alkalinity) was also measured in the field by titration using 0.1N HCl. Repeated analysis of the same sample yielded an internal confidence of 5%. Samples for chemical and isotopic analysis were stored in cleaned polyethylene bottles. For major cations and trace element analyses water samples were filtered using a 0.45 μm nylon filter, and stabilized by ultrapure HNO_3. The concentration of the major ions was determined by liquid chromatography using a Dionex CS-12 and a Dionex AS4A-SC column for cations and anion determinations, respectively. Stable isotope determinations (D/H and $^{18}O/^{16}O$) on water samples were performed by the equilibration technique [Epstein and Mayeda (1953) for oxygen] and water reduction [hydrogen production by using granular Zn, Kendall and Coplen (1985)], respectively. Measurements were carried out using a Finnigan Delta Plus mass spectrometer (hydrogen) and an automatic preparation system coupled with an AP 2003 IRMS (oxygen). The O and H isotopic data are expressed as per mil deviation from the V-SMOW standard (Vienna Standard Mean Oceanic Water) using the conventional $\delta^{18}O$ and δD notation ($\delta=[(R_{sample}/R_{standard})-1]*1000$ (‰) where R represents the $^{18}O/^{16}O$ or $^2H/^1H$ isotopic ratio). Analytical precision for each measurement is better than 0.2 ‰ for $\delta^{18}O$ and 0,5 ‰ for δD.

The $^{87}Sr/^{86}Sr$ isotopic ratio was measured by solid-source thermal ionization mass spectrometry using a VG-Micromass 54E single-collector mass-spectrometer, equipped with a TAU box. The isotopic fractionation due to the mass-dependent differential vaporization of the isotopes was corrected using the $^{86}Sr/^{88}Sr$ normalizing ratio of 0.1194. The data acquisition and reduction follows the procedure of "Analyst" (Ludwig, 1994). The experimental uncertainties on Sr isotope-ratios represent in-run statistics at a 95% confidence level. Repeated analyses of NBS 987 *Sr* isotopic standard gave an average value of $^{87}Sr/^{86}Sr$=0.71025±0.00002 (n=15), and no correction for instrumental bias was applied to the measured ratios.

Rn activity was measured by both a scintillation cell and an ionization chamber (Silena Prassi and Alpha Guard, respectively) with a sensitivity of 4 Bq/m^3. The measurements were carried out following the same procedure of bubbling a 100 ml water sample for ten minutes then taking the value after having left the stripped gas in the measuring cell for three hours. The collected values were corrected from the Rn decay time and expressed in Bq/l.

4.2. Strain in the Friuli area

A seismometric network has been operating in the Friuli area since May 1977, and more than 20,000 earthquakes have been located in these 30 years. For the sites involved in the geochemical measurements, the accumulation in time of the strain, which will be later released as earthquakes, has been computed. The results are given by the time history of seismic strain at the study sites as well as by maps of strain at a certain date.

Table 1 - Location of the sampling sites (see Fig. 1a). The structures where the sampling sites are located are: AT= Alto Tagliamento line; FS=Fella-Sava line; BS=Barcis-Staro Selo line; DA=Mt. Dof-Mt. Auda line; MB=Mt. Bernadia line.

Spring	Longitude E	Latitude N	Structure
Forni (1)	12°38'46.88"	46°23'16.77"	AT
Gemona (2)	13°08'38.20"	46°16'26.69"	BS
Vedronza (3)	13°14'30.72"	46°16'02.10"	BS
Barcis (4)	12°29'53.88"	46°12'26.40"	BS
Putha (5)	12°35'27.00"	46°20'26.16"	DA
Grasia (6)	12°46'36.91"	46°21'57.57"	DA
Lusnizza (7)	13°22'42.28"	46°29'42.81"	FS
Paularo (8)	13°07'26.00"	46°30'46.26"	FS
Patuchis (9)	13°14'23.36"	46°13'41.30"	MB

In detail, strain at the test site locations was computed through the parameters of the G-R relation. The *b*-value was calculated for the seismogenic zone of the FRI zonation of Slejko *et al*. (2008) located in central Friuli from the data of the national historical earthquake catalogue (Gruppo di Lavoro CPTI, 1999, 2004) integrated with the data of the regional seismometric network (OGS, 1977-1981, 1982-1990, 1991-1999, 2000-2010). The value of 1.18 was obtained, considering moment magnitude as earthquake parameter. The *a*-value was obtained from the geodetic regional strain rate, decreased by the amount of estimated aseismic release (equal to 79% in the eastern Alps), and the *b*-value previously defined. In fact, the regional seismic strain rate is equal to the sum of the number of events in each seismic moment class, times the value of the seismic moment itself [see details in Slejko *et al*. (2010)]. Considering that there is a direct relation between moment magnitude classes and seismic moment classes, we have calculated frequencies and recurrence intervals for each magnitude class with these parameters of the G-R relation. The recurrence interval of a certain magnitude class represents the time interval of strain accumulation before the occurrence of the earthquake of that magnitude. The locking depth has been assimilated to the depth of the earthquake: this is a very rough working hypothesis but it should not influence, notably, the final estimates because it likely interests all events evenly.

From the parameters of every earthquake that occurred in the broader Friuli region (from Lake Garda to Ljubljana and from the River Po mouth to the border with Austria), from its recurrence interval, and the regional seismic strain rate, we have derived the strain accumulation time history at the epicentre. Taking into account the distance between the hypocentre and the test site, we have then, computed the strain accumulation time history at the investigated site by Eq. (2) and we have summed up the time histories of all the earthquakes. At the end, we obtained the strain accumulation time history that takes into account all the earthquakes for each studied site that occurred in the broader Friuli region. Though Friuli is dominated by thrusts, it must be pointed out that Eq. (2) applies only for strike-slip faults, that involve only the eastern sector of the study area. As we do not produce absolute estimates of strain but we simply identify the periods of largest strain build up (all strain values in the time histories are normalized), we consider the present approach a rough proxy of the actual seismogenic process.

5. Results

5.1. Regional degassing

The results of the soil degassing measurements have highlighted an unexpected significant CO_2 degassing through the Friuli region (Italiano *et al*., 2009). The degassing rate is higher in its southern sector (northern Friuli Plain) than in the northern one (eastern sector of the Southern Alps). The measured dynamic CO_2 concentrations were always 1-2 orders of magnitude above the atmosphere. The estimated weighted average CO_2 flux of 6 $g·m^{-2}·d^{-1}$ is in the range of the soil biogenic CO_2 source [2-10 $g·m^{-2}·d^{-1}$; Bonan (1995), Morner and Etiope (2002)] or of peatlands located in Slovenia [up to 12 $g·m^{-2}· d^{-1}$; Danevčič *et al*., (2010)]. However, fluxes as high as $3·10^4$ $g·m^{-2}·d^{-1}$, which are several orders of magnitude above any possible biogenic source, have been recorded. The distribution of the peatland deposits over the study area does not match the relevant anomalies in the degassing rate, including both CO_2 and Rn, which are located in coincidence of tectonic lineaments of the investigated area. The δ^{13}C of the CO_2 dissolved in groundwater discharging along fault traces in the eastern Southern Alps (Italiano *et al*., 2009) deviates markedly from the carbon isotopic range of gaseous CO_2 emissions from peats (Charman *et al*., 1999) or from carbonates of the nearby Comacchio area (Cremonini *et al*., 2009). As such, ruling out the atmospheric source, a CO_2-dominated gas phase drained from deep crustal layers superimposes on a background level of organic-derived CO_2. However, possible processes responsible for the local production of inorganic CO_2 have to be considered (e.g., Italiano *et al*., 2009) and further investigations, beyond the aim of this paper, are needed to better understand the role of the gaseous species (mainly CO_2 and Rn) released over the wide area of the Friuli region. The Rn flux ranges from 10 to 10^4 $Bq·m^{-2}·d^{-1}$ and displays a similar distribution pattern as the CO_2. The distribution of the soil degassing of both Rn and CO_2, roughly estimated using ordinary kriging (Fig. 3) displays the highest degassing rate for both gases north of the Fella-Sava lineament and in the northern Friuli Plain, in coincidence with the Maniago and Polcenigo-Maniago lineaments.

The CO_2-Rn barely correlate, supporting the role of CO_2 as carrier gas able to remove Rn released by the rocks during its uprising. Both gases are very soluble in water (510 ml/l STP), so the possibility of detecting an active soil degassing is related to both deep gas upraising and gas-water interactions (GWI). Results of the dissolved gas analysis of waters coming from the whole investigated area (Italiano *et al*., 2009) have shown intense GWI processes with CO_2 dissolution and enrichment of the less soluble gas species in the liquid phase.

5.2. Water geochemistry, O-H-Sr isotopes and Rn

The composition of groundwaters in terms of major ions shows distinctive chemical patterns, which characterize $Ca-Mg-HCO_3$, $Ca-Mg-SO_4$ and $Ca-Mg-HCO_3-SO_4$ hydrofacies in the Piper diagram (Fig. 4). The $Ca-Mg-HCO_3$-type waters are characterized by low salinity (TDS between 0.2 and 0.4 g/l), pH ranging between 7.4 and 8.5 and Eh values markedly positive, typical of oxygenated waters. The emergence temperature is in the range of 9.5-13.3 °C, remaining rather constant during the surveyed period, being much higher than the ambient surface temperature during winter.

These waters are likely to represent aquifers which are primarily comprised in carbonatic rocks, probably transported by diffuse flow through a network of microfractures and rock pores or by conduit flows in karst-type larger openings. They range from equilibrium to supersaturation with calcite. The near saturation with dolomite, calculated for some of the springs, would indicate
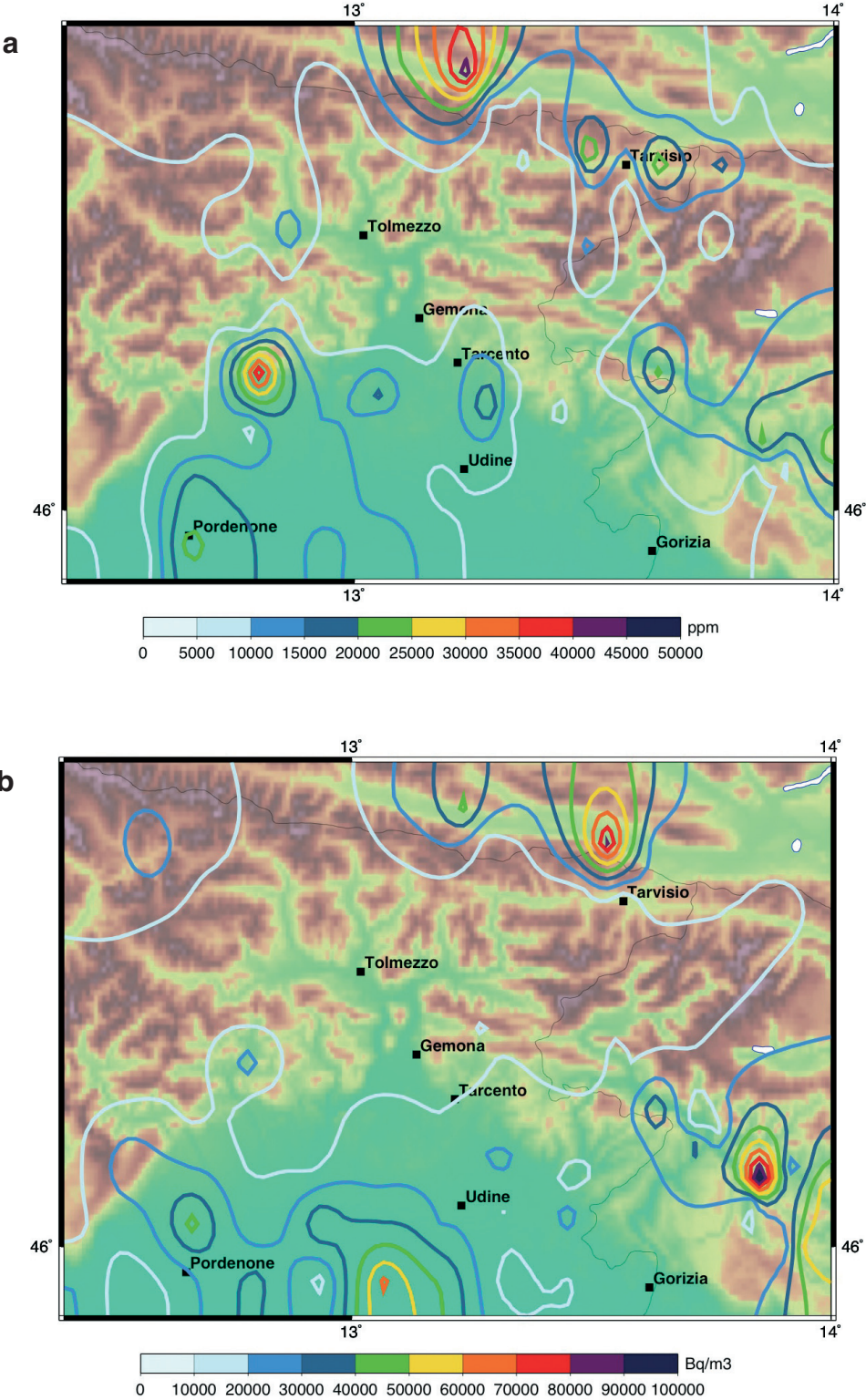
Fig. 3 - Map of the CO_2 (dynamic concentration) (a) and Rn through the soils of the area (b).
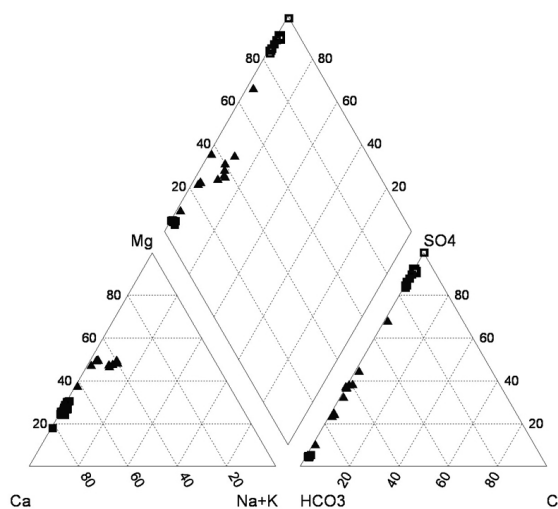
Fig. 4 - Piper diagram used to graphically display the bulk chemical composition of groundwaters. Symbols are: solid square: Ca-Mg-HCO$_3$-type; open square: Ca-Mg-SO$_4$-type; solid triangle: Ca-Mg-HCO$_3$-SO$_4$-type.

long-lasting hydrological circuits of variably CO$_2$ charged waters, allowing the kinetic dissolution of dolomite. Furthermore, these data indicate that carbonate cements may dissolve and re-precipitate at various scales, yielding secondary porosity or low permeability compartments which may be the sites for geopressured fluids.

The Ca-Mg-SO$_4$-type waters show TDS values between 1.5 and 2.5 g/l, pH near-neutral and the redox potential from slightly negative to slightly positive; the Ca-Mg-HCO$_3$-SO$_4$-type waters are characterized by TDS values <1 g/l, pH ranging between 7.3 and 8.5 and the Eh values that are the most negative among the sampled waters. The emergence temperature is in the range of 5.4-13.5 °C for the former type while it is quite constant, clustering to 10 °C and not suffering seasonal variations, for the latter.

Both the Ca-Mg-SO$_4$ and Ca-Mg-HCO$_3$-SO$_4$-type waters are characterized by bacterial sulphate reduction, reflecting a component from pore water devoid of dissolved oxygen.

These waters show the concurrent increase in the concentration of SO$_4^{2-}$, Ca^{2+} and Mg^{2+} which is likely to reflect precipitation/dissolution reactions of calcite, dolomite and gypsum (e.g., Plummer *et al.,* 1990). This indicates a flow through the limestones, dolostone and evaporite layers which characterize the sedimentary sequences in the studied area. In particular, the water chemistry and physico-chemical properties can be modeled equilibrating meteoric water with calcite and dolomite during infiltration, followed by dedolomitization reactions during interactions with gypsiferous layers (e.g., Capaccioni *et al.*, 2001) at relatively high P$_{CO2}$ (P$_{CO2}$ in the range between 10$^{-2.5}$ and 10$^{-1.0}$ atm) and the admixing of a Ca-HCO$_3$ reservoir at depth. However, the Na$^+$/Cl$^-$ molar ratio is usually higher than the 1:1 ratio expected for halite dissolution from evaporite layers, suggesting the possible role of clay minerals in Na$^+$ exchanges. This is also supported by the illite supersaturation observed for some of the waters. The possible role of clays in determining some of the observed geochemical patterns will be addressed in the following.

The δ^{18}O and δD isotopic values for all the water types overlap the meteoric water line reported
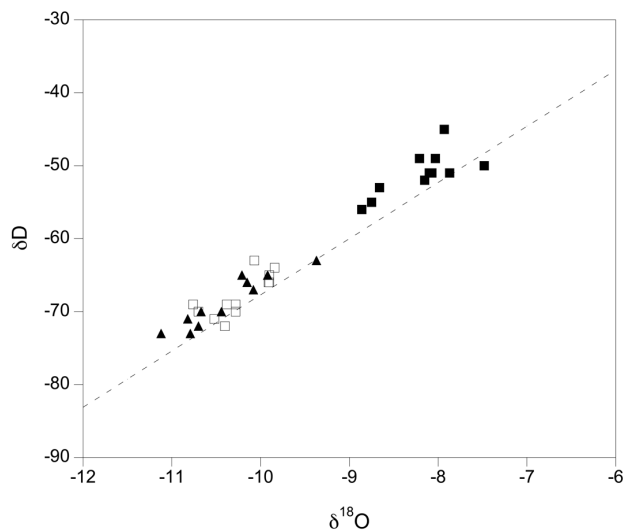
Fig. 5 - Oxygen and hydrogen isotopic composition diagram for the studied groundwaters. Symbols as in Fig. 4. The line for northern Italy precipitations (Longinelli and Selmo, 2003) is also superimposed (dashed line).

for northen Italy (Longinelli and Selmo, 2003), indicating a meteoric origin and the lack of significant evaporation processes prior to infiltration (Fig. 5). The observed distribution of the isotopic data for each of the springs is attributable to the different average elevation of the recharge areas.

Waters from the three different geochemical hydrofacies are also characterized by a variable $^{87}Sr/^{86}Sr$ ratio (usually referred to as *Sr* isotopic composition), as shown in Fig. 6.

Since *Sr* has a non-conservative behaviour, it can be used to trace water-rock interaction processes: the isotopic data support the hypothesis that the different water types represent aquifers which dominantly flow in distinct crustal environments. It is worth noting that the Ca-Mg-SO$_4$ and Ca-Mg-HCO$_3$-SO$_4$ waters deviate towards a more radiogenic signature with respect to that measured on gypsum minerals in evaporites ($^{87}Sr/^{86}Sr$=0.70704±0.00003), reflecting the possible contribution of formation waters (Armstrong *et al.*, 1998) which evolved their $^{87}Sr/^{86}Sr$ ratio through exchanges with Al-silicate minerals. This observation further highlights the possible role of clay minerals, which are commonly found closely associated with gypsum.

The Rn concentrations range from 0.37 Bq/l to 154 Bq/l, with the highest values recorded at the sulphurous Ca-Mg-HCO$_3$-SO$_4$ springs associated with the Barcis-Staro Selo and Alto Tagliamento lineaments.

The Rn$-\delta^{13}$C graph (Fig. 7) remarks the relationships between the regional degassing and the geochemical features of the groundwaters driven to the surface by the local tectonic lines. Gas-water interactions, in fact, drive the CO$_2$ dissolution and change also its isotope composition (Italiano *et al.*, 2009). As CO$_2$ is also the main carrier for Rn, the relationships shown in Fig. 7 agree with different rates of gas-water interactions. The higher the GWI rate, the higher the Rn content and the lower the isotope composition of carbon. The high Rn values recorded in the waters from the sites on the Fella-Sava and Barcis-Staro Selo lines might be a consequence of a stronger degassing activity and agree with their location over the area where anomalous soil CO$_2$ degassing rates, as already stressed.
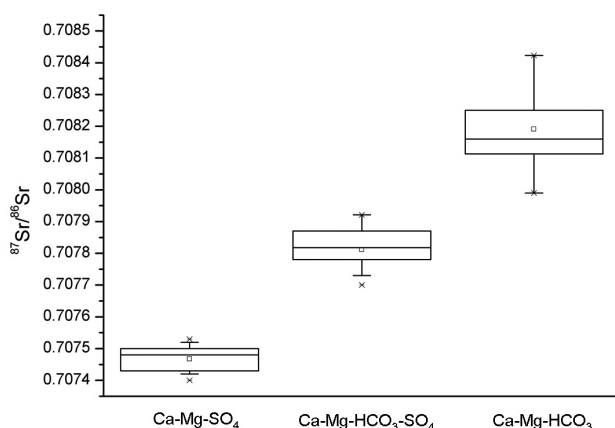
Fig. 6 - Box chart representing the $^{87}Sr/^{86}Sr$ isotopic ratio for the different hydrofacies, suggesting the interaction of waters with different lithologies (see the text).

5.3. Temporal variations and the chloride signal

The whole data set including temperature, pH, Eh, electrical conductivity, bicarbonate, sulphate and chloride ion concentration and Rn activity was evaluated from a statistical point of view, in order to discriminate between random and non-random variations. In a first phase, the data have been analysed by using normal probability plots with the aim of investigating the shape of the frequency distribution, as well as of pointing out the presence of anomalous values. The final target was to identify representative parameters of central tendency (mean or median) and to estimate the features of the variability (Reimann *et al.*, 2008).

Subsequently, the time behaviour for each variable was investigated by using the runs test, a simple robust method able to identify patterns in sequences. The aim was to identify, from a statistical point of view, the presence/absence of random behaviours by comparison with the occurrence of some trend. Under this approach all the variables were represented by the absence or presence of some phenomenon at different points in a sequence, thus obtaining a dichotomous behaviour, having only two possible states, e.g., 1 and 0. A run is consequently defined as a group of adjacent like-states separated by the other states and may have any length, including just one member. If the statistics of the test is z > 1.96 or z < -1.96, the null hypothesis has to be rejected with the 95% level indicating that the sequence shows some non-random pattern or structure. In other words, there are either too few runs of one state or too many runs of the other state for the sequence to be considered random (Borradaile, 2003).

In the case of chloride content, it was easy to obtain a dichotomous sequence, since due to the presence of numerous data at the detection limit the presence or absence of the variable was the only relevant information to be numerically managed. In this framework, data for all the analysed sampling places have revealed a random behaviour both at the year and month scale ($p > 0.05$).

In all the other cases, a dichotomous sequence was obtained by attributing 1 and 0 values to data located below or above the mean or median values. These central tendency values were considered representative of the data set only after having verified the nature of the frequency distribution as reported at the beginning.
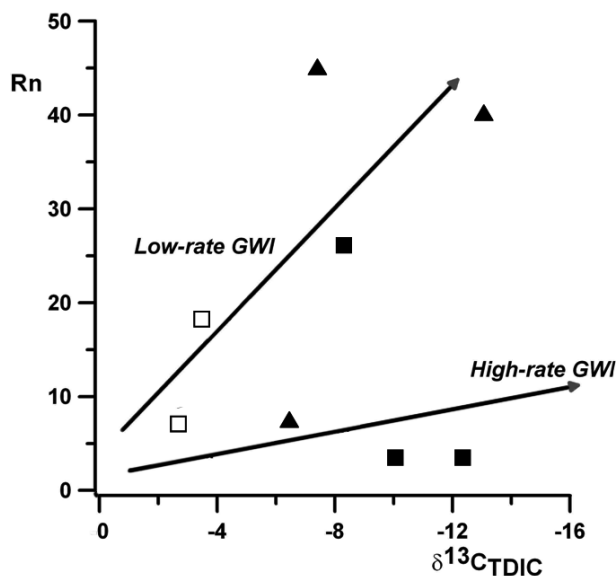
Fig. 7 - Rn vs. isotope composition of TDIC (total dissolved inorganic carbon). The $\delta^{13}C$ TDIC provides the information that CO_2 dissolves in groundwaters following GWI processes at variable extents. The same process allows Rn to dissolve and the different paths shown by the sampled waters are here interpreted as related to different degassing rates. Symbols as in Fig. 4.

Results indicated that temperature, Eh, pH, HCO_3^- and SO_4^{2-} show generally a non random behaviour ($p < 0.05$), which is attributed to seasonal processes and/or mixing between different aquifers at variable extent. It is hence believed that these parameters cannot be used as geochemical tracers of fault-induced processes without some risk. On the contrary, chloride and Rn changes are invariably related to random phenomena, which might reflect transients related to episodic processes in the fault zone overwhelming possible seasonal changes. The patterns obtained for temperature, electrical conductivity, chloride content and Rn activity for some springs are shown in Fig. 8.

The observed chloride geochemical spikes have been evaluated in terms of the possible role of deformation in enhancing mineral reactions involving clays (Huang *et al.*, 1993; Spiess and Bell, 1996). Among such diagenetic reactions, the illitization of dioctahedral smectite with increasing pressure and heating is of particular interest in studying the mechanical properties and strength of faults: the evolution of precursor smectite to illite strongly decreases the gauge permeability (e.g., Jiao and Surdam, 1997), also producing quartz cement, liberates large volumes of interlayer waters and releases considerable amounts of ions (e.g., Na^+). In addition, illite and other clay minerals may participate in silicate-carbonate reactions, producing CO_2 (Hutcheon and Desrocher, 2003) which dissolves in water and precipitates carbonate minerals or, if its solubility product is exceeded, forms a free gas phase which produces abnormally high fluid pressure within the sealed rock pores. The increase in permeability and the formation of a fracture network along compressive structures in response to strain changes may result in the expulsion of such pore fluids, which move rapidly from the overpressured to the hydropressured zones of the fault gauge. In high permeability systems, large amounts of these fluids may be vertically transported to the surface and contribute to shallower aquifers, yielding short-living chemical zonations that are recorded at the spring site.

Since clays have a negative surface charge, anions such as Cl^- are confined to only a part of the pore spaces; during deformation and compaction, the chloride is expelled and its
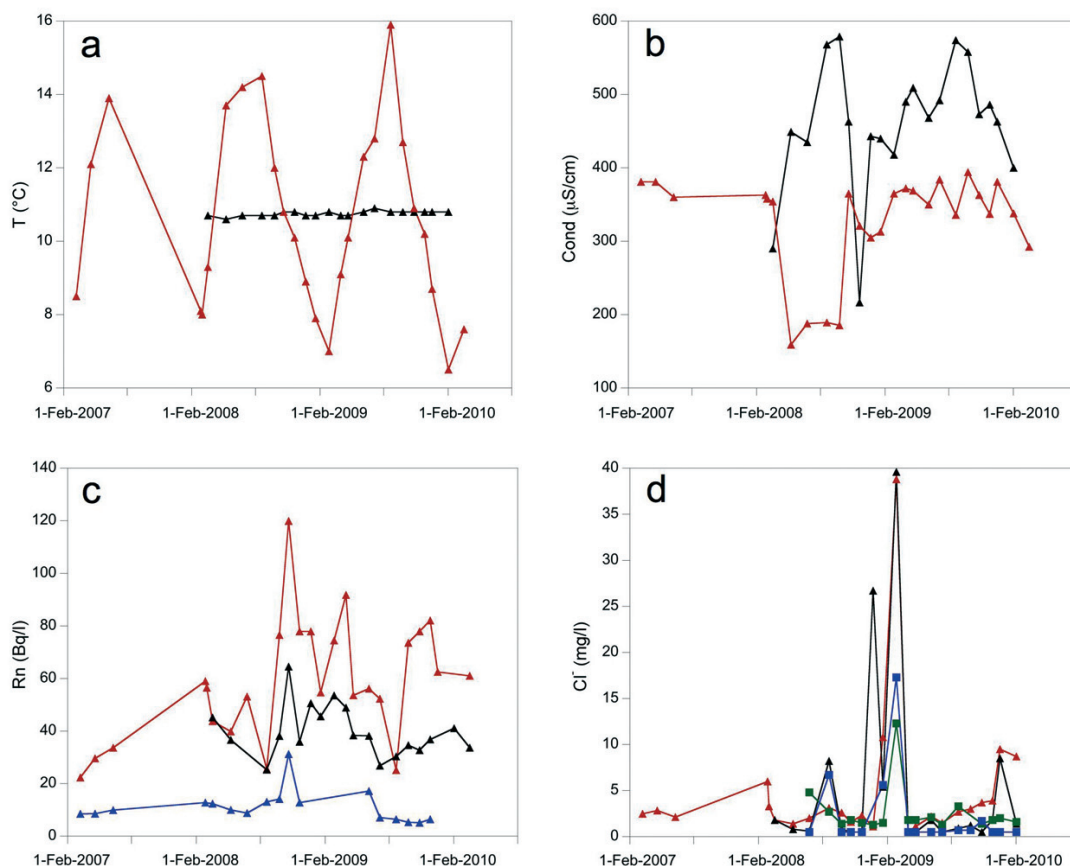
Fig. 8 - Patterns for temperature (a), electrical conductivity (b), Rn activity (c) and chloride content (d) for some springs related to the Barcis-Staro Selo (red line), Alto Tagliamento (black line), Mt. Dof-Mt. Auda (blue line), and Mt. Bernadia (green line) lineaments. Symbols as in Fig. 4.

concentration in the pressure effluent which begins to flow may become higher than in the original solution.

This process has been quantified in terms of the Gouy-Chapman theory of the diffuse double layer (DDL) and the Donnan equilibrium during compaction of a clay suspension (Appelo, 1977).

In the DDL model, the distribution of the electric potential Ψ (in Volt) in the pore solution as a function of the distance x from a charged surface is given by (Appelo and Postma, 2005):

$$\left(\frac{d\psi}{dx}\right)^2 = 2\left(\frac{RT}{\varepsilon}\right)m_{i,\infty}\left[\exp\left(-\frac{F\psi}{RT}\right)+\exp\left(-\frac{F\psi}{RT}\right)-2\right] \qquad (3)$$

where ε is the dielectric constant of water, F, Faraday's constant, T the temperature (K) and R the gas constant. The concentration m (actually activity) of a given ion in the electric field is given by Boltzman's equation:

$$\frac{m_{Cl_o}}{m_{Cl,x_1}} = \exp\left(\frac{-z_i F \psi_a}{RT}\right) / \exp\left(\frac{-z_i F \psi_b}{RT}\right) \qquad (4)$$

where the subscript o and x_1 refer to the position in the field. Eq. (3) was integrated and the chloride concentrations calculated as a function of x using Eq. (4). The thickness of the DDL was calculated on the basis of the actual ionic strength of the water. The cation exchange capacity reported in the literature for illite has been used.

The observed sharp increase in the Cl^- concentration observed for some of the springs can be quite satisfactorily fitted within this model. As an example, the chloride spike recorded by the Ca-Mg-HCO_3-SO_4 waters located along the Barcis-Staro Selo can be accounted for by admixing to the water reservoir about the 2 vol % of a leaked pore fluid obtained after about 98% compaction of an illite suspension, starting from an initial concentration in the suspension of about $2 \cdot 10^{-5}$ mol/l as obtained by Eqs. (3) and (4) for a water film having the thickness corresponding to the overlap of the double layers. It is, however, worthy of note that other solutions are numerically possible, and additional constraints will be necessary in the modeling of the chloride transients.

6. Discussion

The results provided by the investigations on soil degassing, besides the geochemical features of the collected groundwaters, coherently show that a regional release of deep-originated, CO_2-dominated gases involves the seismic area of the Friuli-Venezia Giulia region. The gas phase is driven to the surface by the local tectonic lines and interacts with the groundwaters circulating at different crustal levels, dissolving significant amounts of CO_2 and Rn. Even if groundwaters display variable geochemical features, as they equilibrated in different geological units, they underwent the same process of gas-water interaction although at different extents. Following the above-mentioned information, we can sketch the following model for fault-fluids interactions over the region: deeply originating CO_2-dominated fluids of crustal origin rise toward the surface following the main structural discontinuities, namely the main tectonic lines. The uprising fluids interact with groundwaters located at different levels inside the shallow crust and equilibrated with different hosting rocks. The GWI allows dissolution of the most soluble species (e.g., CO_2 and Rn) and changes the geochemical features of the gas phase because of chemical and isotope fractionation processes.

Such a simple model schematizes the fault-fluids interactions in a steady state condition. Poroelastic responses to seismic wave energy and variations in the strain and stress field are a commonly accepted interpretation for fluid-related anomalies, and hydrological responses to local seismicity have been reported (e.g., Muir-Wood and King, 1993; Rojstaczer *et al*., 1995; Gasparini *et al*., 2002) often interpreted as consequences of fault-valve effect on the circulating fluids. Irrespective of the occurrence of any earthquake, the active tectonics of the area induces compressional and strike-slip state of stress and rock deformation. The geochemical features of fluids involved in such an unstable environment change since they try to re-equilibrate because of modifications of the boundary conditions of the hosting rocks. During this transient phase, they

display temporal variations in some chemical parameters, as recorded by springs along the Alto Tagliamento and the westernmost sector of the Barcis-Staro Selo lineaments. In our study-case, episodic expulsion of such pore waters related to the break of low permeability barriers might explain some of the observed temporal chloride and Rn changes.

The earthquake instability in response to remote tectonic loading is preceded by precursory slip weakening usually accompanied by microcracking and deformation of the rock surrounding the fault, which produces a deviation of the strain-rate from the background level (Rudnicki, 1988). Even if the dilatancy accompanying the slip is typically small, it may be significant in terms of pore diffusion into newly created void spaces (e.g., Rudnicki and Chen, 1988) and in causing gases to come out of the solution. In addition, the balance between pore fluid diffusion rate and dilatancy affects the effective stress, given by the total stress minus pore pressure, on the slip surface.

The relationships between the calculated strain and the measured changes in Rn activity and chloride concentration in springs related to the Alto Tagliamento, Barcis-Staro Selo, and Mt. Dof-Mt. Auda lineaments are graphically shown in Fig. 9. It is observed that the spikes in chloride concentration shortly follow or are concomitant with the abrupt change in the strain; Rn activity also shows variations which in some cases seem to precede or be concurrent with strain release.

The time correspondence between strain and geochemical signals, the short-living character of the chloride and Rn geochemical transients and the lack of a corresponding increase in the outlet temperature of springs suggest that the observed hydrological phenomena are likely confined to relatively superficial sources. It has however to be noted that the strain could occur at a higher depth, finding direct routes to the surface and affecting springs even located at some distance. Furthermore, it was seen that some wells in Japan change sensitivity with time, reflecting changes in regional stress in the area (Wakita, 1996). The model proposed to account for the observed chloride concentration spikes is consistent with fault displacement vectors yielding a resulting strain changing from compressional during the first deformative phases to dilatational (Carrigan *et al.*, 1991), and could mimic the regional strain field.

7. Conclusions

The perennial springs attributable to long-lasting circulation in different networks of seismogenic fractures of the Friuli-Venezia Giulia region (NE Italy) have been investigated for the first time with the aim of better understanding the relationships between fluids and tectonics, coupling different ways of modeling the geochemical features of the liquid phase and strain accumulation and release.

A stress accumulation may have generated an increase in fluid transport towards the surface along the existing migration paths of the fault line. Trapped fluids could be activated by a temporary increase of hydraulic conductivity by dilatancy and microfracturing. Pore pressure diffusion, as a subsequent process, transmits this signal towards the surface and could be also responsible for triggering single seismic events on that fault plane. This process in the upper crust is linked to existing fluid transport paths towards the surface. The nature of soil degassing indicates a deep origin of the gases, possibly related to calcite decomposition by friction processes producing lime and CO_2 along the slip planes of tectonically active structures. CO_2 carries Rn from deep sources towards the surface, where it partitions into groundwaters which migrate at shallower crustal depth. The clayed components of the fault gauges are proposed as having an active role in participating in mineral
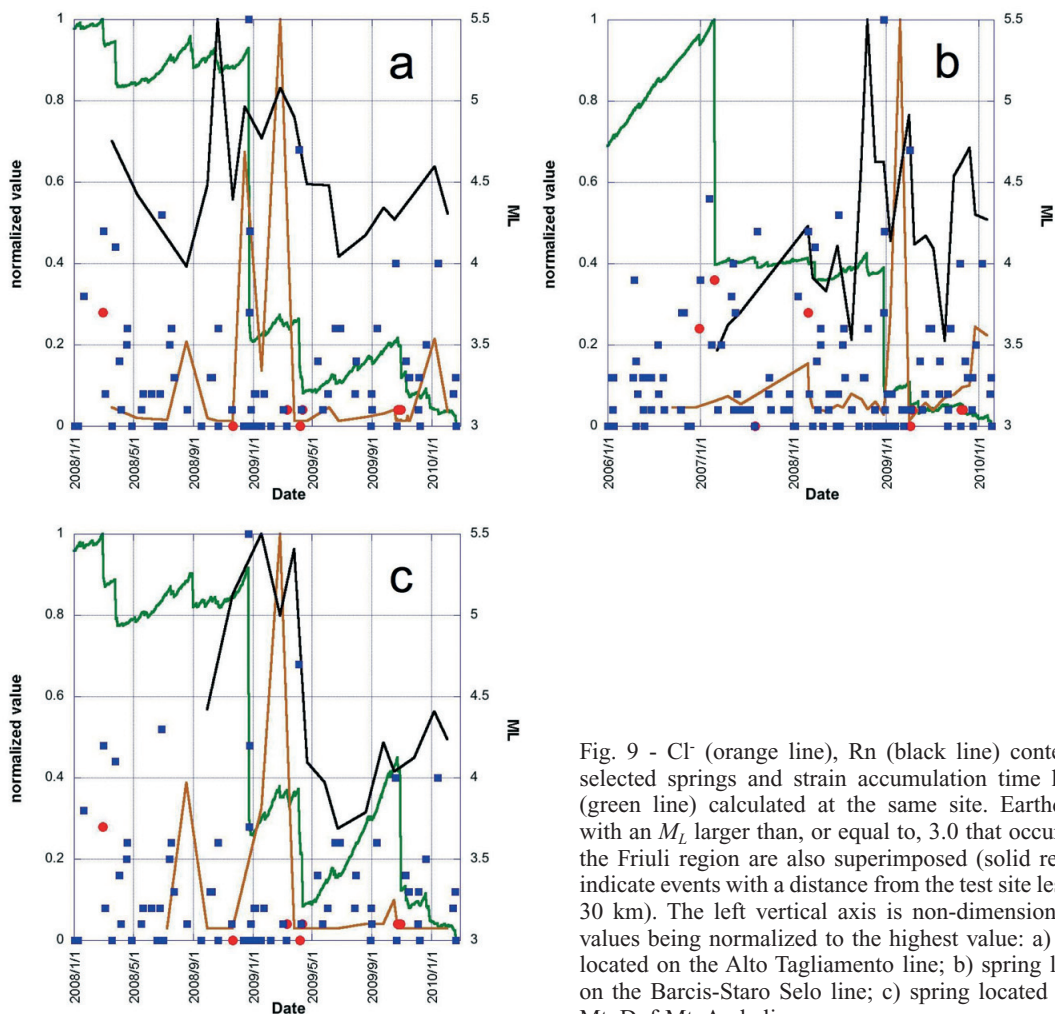
Fig. 9 - Cl⁻ (orange line), Rn (black line) content for selected springs and strain accumulation time history (green line) calculated at the same site. Earthquakes with an M_L larger than, or equal to, 3.0 that occurred in the Friuli region are also superimposed (solid red dots indicate events with a distance from the test site less than 30 km). The left vertical axis is non-dimensional, the values being normalized to the highest value: a) spring located on the Alto Tagliamento line; b) spring located on the Barcis-Staro Selo line; c) spring located on the Mt. Dof-Mt. Auda line.

reactions possibly catalyzed by deformation, and in selectively releasing ions from pores during compaction. The observed spikes in chloride concentration are interpreted as related to filtration processes associated with compaction, and in this sense chloride and Rn are intended as sensitive indicators of earthquake strain.

The collected results suggest that any geochemical monitoring should not look for a direct earthquake-geochemical variation relationship, but an innovative approach has to be adopted since anomalies do not appear to be necessarily linked to seismic events, but rather to the seismogenic process related to geodynamical processes over a larger zone.

REFERENCES

Appelo C.A.J.; 1977: *Chemistry of water expelled from compacting clay layers: a model based on Donnan equilibrium.* Chem. Geol., **19**, 91-98.

Appelo C.A.J. and Postma D.; 2005: *Geochemistry, groundwater and pollution. 2nd edition.* A.A. Balkema Publ., Dordrecht, 655 pp.

Armstrong S., Sturchio N. and Hendry M.J.; 1998: S*trontium isotopic evidence on the chemical evolution of pore waters in the Milk River aquifer, Alberta, Canada.* Applied Geochem., **13**, 463-476.

Bonan G.B.; 1995: *Land-atmosphere CO_2 exchange simulated by a land surface process model coupled to an atmospheric general circulation model.* Journal of Geophysical Research, **100**, 2817-2831.

Borradaile G.; 2003: *Statistics of Earth science data.* Springer-Verlag, 351 pp.

Bressan G., Snidarcig A. and Venturini C.; 1998: *Present state of tectonic stress of the Friuli area (eastern Southern Alps).* Tectonophysics, **292**, 211–227.

Capaccioni B., Didero M., Paletta C. and Salvadori P.; 2001: *Hydrogeochemistry of groundwaters from carbonate formations with basal gypsiferous layers: an example from the Mt Catria-Mt Nerore ridge (Northern Apennines, Italy).* J. Hydrol., **253**, 14-26.

Carapezza M.L. and Granieri D.; 2004: *CO_2 soil flux at Vulcano (Italy): comparison between active and passive methods.* Appl. Geochem., **19**, 73-88.

Carrigan C.R., King G.C.P., Barr G.E. and Bixler N.E.; 1991: *Potential for water-table excursions induced by seismic events at Yucca Mountains, Nevada.* Geology, **19**, 1157-1160.

Carulli G.B.; 2006: *Carta geologica del Friuli Venezia Giulia, scala 1:150.000.* Regione Autonoma Friuli Venezia Giulia, Direzione Regionale Ambiente e Lavori Pubblici, Servizio Geologico Regionale.

Carulli G.B. and Ponton M.; 1992: *Interpretazione strutturale profonda del settore centrale carnico-friulano.* Studi Geol. Camerti, vol. 2 CROP 1-1A, 275-284.

Carulli G.B., Cozzi A., Longo Salvador G., Pernacic E., Podda F. and Ponton M.; 2000: *Geologia delle Prealpi Carniche.* Museo Friul. St. Nat., pubbl. n. 44, Udine, 48 pp.

Carulli G.B., Longo Salvador G., Poli E., Ponton M., Tunis G., Vaia F. and Venturini C.; 2002: *Itinerario n° 7: Da Udine a Sella Nevea.* In: Vai G.B., Venturini C., Carulli G.B. and Zanferrari A. (eds), Alpi e Prealpi Carniche e Giulie, Guide Geol. Reg., Soc. Geol. It., vol. 9, pp. 269-297.

Cavallin A. and Martinis B.; 1982: *Gli scorrimenti del margine settentrionale della Piattaforma Carbonatica Adriatica.* In: Castellarin A. and Vai G.B. (eds), Guida alla Geologia del Sudalpino centro-orientale, Guide Geol. Reg., Soc. Geol. It., Bologna, pp. 349- 359.

Charman D.J., Aravena R., Bryant C.L. and Harkness D.D.; 1999: *Carbon isotopes in peat, DOC, CO_2 and CH_4 in Holocene peatland on Dartmoor, southwest England.* Geology, **27**, 539-542.

Cheloni D., Mantenuto S., D'Agostino N., Hunstad I. and Selvaggi G.; 2004: *Cinematica e deformazione attiva della regione padano – adriatica.* In: Slejko D. and Rebez A. (eds), Gruppo Nazionale di Geofisica della Terra Solida, 23° Convegno Nazionale, Riassunti estesi delle comunicazioni, Tipografia Mosetti, Trieste, pp. 32-35.

Cremonini S., Etiope G., Italiano F. and Martinelli G.; 2008: *Evidence of possible enhanced peat burning by deep-origin methane in the Po river delta plain (Italy).* Journal of Geology, **116**, 401-413.

Danevčič T., Mandic-Mulec I., Stres B., Stopar D. and Hacin J.; 2010: *Emissions of CO_2, CH_4 and Na_2O from Southern European peatlands.* Soil Biology & Biochemistry, **42**, 1437-1446.

Epstein S. and Mayeda T.K.; 1953: *Variations of the $^{18}O/^{16}O$ ratio in natural waters.* Geochim. Cosmochim. Acta, **4**, 213-224.

Galadini F., Poli M.E. and Zanferrari A.; 2005: *Seismogenic sources potentially responsible for earthquakes with M > 6 in the Eastern Southern Alps (Thiene-Udine sector, NE Italy).* Geoph. Jour. Int., **161**, 739-762.

Gasparini C., Di Mauro R., Agliuca N.M., Pirro M. and Marchetti A.; 2002: *Recent seismicity of the "Acque Albule" travertine basin.* Annals of Geophysics, **45**, 537-550.

Gruppo di Lavoro CPTI (Boschi E., Gasperini P., Valensise G., Camassi R., Castelli V., Stucchi M., Rebez A., Monachesi G., Barbano M.S., Albini P., Guidoboni E., Ferrari G., Mariotti D., Comastri A. and Molin D.); 1999: *Catalogo Parametrico dei Terremoti Italiani.* ING, GNDT, SGA, Bologna, 92 pp.

Gruppo di lavoro CPTI; 2004: *Catalogo Parametrico dei Terremoti Italiani, versione 2004 (CPTI04).* INGV, Bologna, http://emidius.mi.ingv.it/CPTI04/.

Gurrieri S. and Valenza M.; 1988: *Gas transport in natural porous mediums: a method for measuring CO_2 flows from the ground in volcanic and geothermal areas.* Rend. Soc. It. Mineral. Petrol, **43**, 1151–1158.

Gutenberg B. and Richter C.F.; 1944: *Frequency of earthquakes in California.* Bull. Seism. Soc. Am., **34**, 185-188.

Huang W.-L., Longo J.M. and Pevear D.R.; 1993: *An experimentally derived kinetic model for smectite-to-illite conversion and its use as a geothermometer Clay.* Clay Mineral., **41**, 162-177.

Hutcheon J. and Desrocher S.; 2003: *Silicate-carbonate reactions in sedimentary systems: fluid composition contro, and potential for generation of overpressures.* In: Worden R.H. and Morad S. (eds), Clay mineral cements in sandstones, Blackwell Publishing, pp. 161-176.

Italiano F., Bonfanti P., Ditta M., Petrini R. and Slejko F.; 2009: *Helium and carbon isotopes in the dissolved gases of Friuli region (NE Italy): geochemical evidence of CO_2 production and degassing over a seismically active area.* Chem. Geol., **266**, 76–85.

Jiao Z.S. and Surdam R.C.; 1997: *Characteristics of anomalously pressured Cretaceous shales in the Laramide basins of Wyoming.* In: Surdam R.C. (ed), Seals, traps and the petroleum system, AAPG Memoir 67, The American Association of Petroleum Geologists, Tulsa Oklahoma U.S.A., pp. 243– 253.

Kendall C. and Coplen T.B.; 1985: *Multisample conversion of water to hydrogen by zinc for stable isotope determination.* Analytical Chemistry, **57**, 1437–1440.

Longinelli A. and Selmo E.; 2003: *Isotopic composition of precipitation in Italy: a first overall map.* J. Hydrol., **270**, 75-80.

Ludwig K.R.; 1994: *Analyst. A computer program for control of a thermal-ionization single-collector mass-spectrometer.* Open-file report 92-543, U.S.G.S., Berkeley California U.S.A., 95 pp.

Merlini S., Doglioni C., Fantoni R. and Ponton M.; 2002: *Analisi strutturale lungo un profili geologico tra la linea Fella-Sava e l'avampaese adriatico (Friuli Venezia Giulia-Italia).* Mem. Soc. Geol. It., **57**, 293-300.

Mogi K.; 1985: *Earthquake prediction.* Academic Press, Tokyo, 355 pp.

Morner N.A. and Etiope G.; 2002: *Carbon degassing from the lithosphere.* Global Planet. Change, **33**, 185-203.

Muir-Wood R. and King G.C.P.; 1993: *Hydrological signatures of earthquake strain.* J. Geophys. Res., **98**, 22035-22068.

OGS; 1977-1981: *Bollettino della Rete Sismologica del Friuli Venezia Giulia.* OGS, Trieste.

OGS; 1982-1990: *Bollettino della Rete Sismometrica dell'Italia Nord-Orientale.* OGS, Trieste.

OGS; 1991-1999: *Bollettino della Rete Sismometrica del Friuli Venezia Giulia.* OGS, Trieste.

OGS; 2000-2010: *Friuli Venezia Giulia Network Localized Events.* www.crs.inogs.it/bollettino/RSFVG/RSFVG.it.html.

Pizzino L., Burrato P., Quattrocchi F. and Valensise G.; 2004a: *Geochemical signatures of large active faults: the example of the 5 February 1783, Calabrian earthquake (southern Italy).* J. Seismology, **8**, 363-380.

Pizzino L., Quattrocchi F., Cinti D. and Galli G.; 2004b: *Fluid geochemistry along the Eliki and Aigion seismogenic segments (Gulf of Corinth, Greece).* C.R. Geoscience, **336**, 367-374.

Plummer L.N., Busby J.F., Lee R.W. and Hanshaw B.B.; 1990: *Geochemical modeling of the Madison Aquifer in parts of Montana, Wyoming and South Dakota.* Water Resour. Res., **26**, 1981-2014.

Poli M.E.; 1996: *Analisi strutturale del Monte di Medea (Friuli): tettonica polifasica nell'avampaese sudalpino orientale.* Atti Ticinensi di Scienze della Terra, Serie Speciale, **4**, 103-113.

Ponton M.; 2008: *Note geologiche sulle Prealpi Giulie nord-occidentali.* Mem. Ist. It. Spel., **20**, 53-71.

Reimann C., Filzmoser P., Garret R. and Dutter R.; 2008: *Statistical data analysis explained.* John Wiley & Sons Ltd,

England, 343 pp.

Riggio A. and Sancin S.; 1986: *Variazione nel tempo del parametro b quale precursore.* In: Atti del 5° Convegno GNGTS, Esagrafica, Roma, pp. 407-419.

Riggio A., Sancin S., Santulin M., Popit A., Vaupotic J. and Zmazek B.; 2003: *Radon e sismicità in Italia nord-orientale.* In: Atti del 22° Convegno Nazionale GNGTS, file /06.26, Prospero, Trieste, CD-Rom.

Riggio A., Santulin M., Slejko F., Ditta M. and Italiano F.; 2007: *Geochemical monitoring of fluids in proximity of seismogenetic structures.* In: Gruppo Nazionale di Geofisica della Terra Solida, 26° Convegno Nazionale, Riassunti Estesi delle Comunicazioni, Stella Arti Grafiche, Trieste, pp. 54-57.

Roeloffs E.; 1999: *Radon and rock deformation.* Nature, **399**, 104-105.

Rojstaczer S., Wolf S. and Michel R.; 1995: *Permeability enhancement in the shallow crust as a cause of earthquake-induced hydrological changes.* Nature, **373**, 237–239.

Rudnicki J.W.; 1988: *Physical models of earthquake instability and precursory processes.* PAGEOPH, **126**, 531-553.

Rudnicki J.W. and Chen C.H.; 1988: *Stabilization of rapid frictional slip on a weakening fault by dilatant hardening.* J. Geophys. Res., **93**, 4745-4757.

Scholz C.H., Sykes L.R. and Aggarwal Y.P.; 1973: *Earthquake prediction: a physical basis.* Science, **181**, 803-810.

Sibson R.H.; 1990: *Conditions for fault-valve behaviour.* In: Knipe R.J. and Rutter E.H. (eds), Deformation mechanisms, rheology and tectonics, Geol. Soc. London, Spec. Pubbl. 5G, pp. 15-28.

Slejko D., Caporali A., Stirling M. and Barba S.; 2010: *Occurrence probability of moderate to large earthquakes in Italy based on new geophysical methods.* J. Seismol., **14**, 27-51, doi: 10.1007/s10950-009-9175-x.

Slejko D., Carulli G.B., Nicolich R., Rebez A., Zanferrari A., Cavallin A., Doglioni C., Carraro F., Castaldini D., Iliceto V., Semenza E. and Zanolla C.; 1989: *Seismotectonics of the eastern Southern-Alps: a review.* Boll. Geof. Teor. Appl., **31**, 109-136.

Slejko D., Rebez A. and Santulin M.; 2008: *Seismic hazard estimates for the Vittorio Veneto broader area (N.E. Italy).* Boll. Geof. Teor. Appl., **49**, 329-356.

Spiess R. and Bell T.H.; 1996: *Microstructural controls on sites of metamorphic reaction; a case study of the inter-relationship between deformation and metamorphism.* Eur. J. Mineral., **8**, 165-186.

Stein S. and Wysession M.; 2003: *An introduction to seismology, earthquakes, and Earth structure.* Blackwell Publishing, Oxford, 498 pp.

Sukhija B.S., Reddy D.V., Nagabhushanam P. and Kumar B.; 2010: *Significant temporal changes in ^{13}C in dissolved inorganic carbon of groundwater related to resevoir-triggered seismicity.* Seism. Res. Lett., **81**, 218-224.

Talamo R., Pampaloni M. and Grassi S.; 1978: *Risultati delle misure di livellazione di alta precisione eseguite dall'Istituto Geografico Militare nelle zone del Friuli interessate dalle recenti attività sismiche.* Boll. Geod. Sc. Aff., **37**, 61-75.

Toutain J.P. and Baubron J.C.; 1999: *Gas geochemistry and seismotectonics: a review.* Tectonophysics, **304**, 1-27.

Ulomov V.I. and Mavashev B.Z.; 1971: *Forerunner of Taskent earthquakes.* Izn. Akad. Nauk Uzb. USSR, 188-200.

Venturini C.; 1990. *Cinematica neogenico-quaternaria del Sudalpino orientale (settore friulano).* Studi Geol. Camerti, Vol. Spec. 1990, 109-116.

Virk H.S., Walia V., Kumar Sharma A., Kumar N. and Kumar R.; 2000: *Correlation of radon anomalies with microseismic events in Kangra and Chamba valleys of N-W Himalaya.* Geofísica Internacional, **39**, 221-227.

Wakita H.; 1996: *Geochemical challenge to earthquake prediction.* In: Proc. Nat. Acad. Sci. USA, vol. 93, pp. 3781-3786.

Zanferrari A.; 2003: *The external thrust-belt of the Eastern Southern Alps in Friuli (NE Italy).* Mem. Sci. Geol., **54**, 159-162.

Corresponding author: Riccardo Petrini
                            Dipartimento Geoscienze, Università di Trieste
                            Via Weiss 8, 34100 Trieste, Italy
                            Phone: +39 040 5582223; fax: +39 0405582213; e-mail: petrini@units.it